https://doi.org/10.5194/egusphere-2025-3493
Preprint. Discussion started: 14 August 2025

Future hydro-climatic changes associated with global warming and stratospheric aerosol intervention scenarios across Central-South Asia and the Tibetan Plateau

Azfar Hussain[1,2], Abolfazl Rezaei[3], Ping Zhu [1], Guanglang Xu[1], Chao Yang [2], Yan Ma[1], Tianye Cao[1], Huizeng Liu[1,2,*]

[1] Institute for Advanced Study & Tiandu-Shenzhen University Deep Space Exploration Joint Laboratory & Space Science Center, Shenzhen University, Shenzhen 518060, China

[2] MNR Key Laboratory for Geo-Environmental Monitoring of Great Bay Area & Guangdong Key Laboratory of Urban Informatics & Shenzhen Key Laboratory of Spatial Smart Sensing and Services, Shenzhen University, Shenzhen 518060, China

[3] Department of Earth Sciences, Institute for Advanced Studies in Basic Sciences, Zanjan 45137–66731, Iran

Corresponding: Huizeng Liu, Institute for Advanced Study, Shenzhen University, Shenzhen 518060, China

[*] Corresponding author, E-mail: huizeng.liu@szu.edu.cn

https://doi.org/10.5194/egusphere-2025-3493
Preprint. Discussion started: 14 August 2025

ABSTRACT

The Central and South Asian Tibetan Plateau (CSATP) plays a vital role in regulating regional and downstream water availability. However, the region faces growing threats from global warming-induced hydroclimatic changes. This study investigates the hydro-climatic changes in the CSATP region under two future (2071-2100) scenarios of high greenhouse gas (GHG) emissions (SSP5-8.5) and the combined impact of GHG with stratospheric aerosol intervention (SAI), relative to present-day conditions (2015-2035). The temperature, precipitation, real evapotranspiration (RET), available water (AW), runoff, soil moisture (SM), terrestrial water storage (TWS), and leaf area index (LAI) are assessed using model simulations from CESM2-WACCM. These variables exhibit widespread intensification, with significant increases in temperature, precipitation, runoff, and LAI, particularly in eastern central Asia (ECA) and South Asia (SA), accompanied by enhanced seasonal amplitudes and earlier runoff peaks. These shifts indicate stronger seasonality and heightened extremes across the land surface. In contrast, the Geo SSP5-8.5 1.5 (here called Geo-SAI) scenario effectively reduces temperature and dampens the seasonal amplitude of TWS, runoff, RET, and precipitation, thereby counteracting many GHG-emission induced changes. However, Geo-SAI also amplifies seasonal variability in SM and vegetation (LAI), especially in ECA and the Tibetan Plateau (TP), revealing its regionally heterogeneous impacts on land–atmosphere interactions under solar geoengineering. While Geo-SAI doesn't fully eliminate impacts, it offers a promising route to reduce extremes and enhance climate stability in vulnerable regions. These findings underscore SAI's potential to ease adverse hydroclimatic effects of GHG-induced warming and support water resource sustainability under high-emission pathways in CSATP.

https://doi.org/10.5194/egusphere-2025-3493
Preprint. Discussion started: 14 August 2025

1. Introduction

Stratospheric aerosol injection (SAI)—a leading solar radiation modification (SRM) strategy has gained increasing attention as a potential means to offset greenhouse gas (GHG)-induced global warming (Crutzen, 2006; Irvine and Keith, 2020; Ricke et al., 2023; Tilmes et al., 2018). By injecting reflective particles into the stratosphere, SAI seeks to mimic the cooling effects of volcanic eruptions and restore Earth's energy balance (Pope et al., 2012; Weisenstein et al., 2015). Model simulations show that SAI can lower global temperatures, but may also introduce complex and regionally uneven hydroclimatic effects, particularly in sensitive regions (Kravitz et al., 2013b; Simpson et al., 2019; Jones et al., 2016; Visioni et al., 2020).

The Central-South Asia and Tibetan Plateau (CSATP) is a climate hotspot, where rapid warming, shifting monsoon dynamics, and intensifying hydroclimatic extremes threaten water security, agriculture, and ecosystems (Kim and Bae, 2020; Stevenson et al., 2022; Ji et al., 2018). The Tibetan Plateau (TP), known as the "Third Pole," is especially vulnerable due to its role in regulating large-scale atmospheric circulation and freshwater availability (Li et al., 2022; Lin et al., 2023). Observations show a decline in terrestrial water storage (TWS) at ~10.2 Gt/year (2002–2017) across the TP (Li et al., 2022), with lake expansion and altered precipitation patterns projected under high-emissions scenarios (Chen et al., 2022; Zhu et al., 2025). Under continued GHG emissions (SSP5-8.5), warming of up to 4.8°C by 2100 is expected (Effiong and Neitzel, 2016), driving intensified extremes including droughts, floods, and shifts in soil moisture (SM), evapotranspiration (ET), and runoff (Samaniego et al., 2018; Naumann et al., 2021; Vicente-Serrano et al., 2020). In South Asia (SA), these changes are already contributing to declining glacier mass (Kraaijenbrink et al., 2017), altered monsoon patterns vulnerabilities exist across Central Asia (CA), where warming and glacier retreat in the Tianshan–Pamir ranges are compounding regional water scarcity (Huang et al., 2021; Fallah et al., 2024; Yu et al., 2021).

SAI has been proposed as a supplementary tool to temporarily offsetting some of the increase in surface temperatures—even under continued high emissions (Visioni et al., 2020). For example, the Geoengineering Model Intercomparison Project (GeoMIP)

https://doi.org/10.5194/egusphere-2025-3493
Preprint. Discussion started: 14 August 2025

scenario Geo SSP5-8.5 1.5 (hereafter "Geo-SAI") aims to stabilize temperatures at ~1.5°C despite following an SSP5-8.5 emissions pathway (Tilmes et al., 2020b). However, while SAI could reduce global warming, its side effects—particularly on precipitation, runoff, and vegetation—remain uncertain and may exacerbate water stress in monsoon and arid regions (Robock et al., 2008; Niemeier and Schmidt, 2017; Cheng et al., 2019; Liu et al., 2024; Simpson et al., 2019; Macmartin et al., 2017). Studies suggest SAI may weaken the hydrological cycle, leading to reduced precipitation and altered runoff generation via changes in land-atmosphere feedbacks, including vegetation dynamics and snowmelt fluxes (Rezaei et al., 2025; Dagon and Schrag, 2019). These effects are especially critical in CSATP, where orography and monsoon circulation create sharp hydroclimatic gradients and interannual variability modulated by spring snow cover, soil moisture, and ENSO-related SST anomalies (Zhu et al., 2023; Wang et al., 2008). Despite growing literature on SAI, major gaps remain in understanding its regional impacts on hydrological processes across CSATP. Past studies have largely focused on global or zonal precipitation changes (Kravitz et al., 2013a; Bala et al., 2008; Huynh and Mcneill, 2024; Schiferl et al., 2018), while fewer have examined vegetation and water storage responses—key mediators of hydroclimate extremes (Clark et al., 2023; Schiferl et al., 2018).

This study addresses these gaps by analyzing future hydroclimatic variability across CSATP under two scenarios: the baseline high-emissions SSP5-8.5 and the SAI-modified Geo-SAI (SSP5-8.5+SAI). Using outputs from the GeoMIP experimental framework, we assess changes in key variables—temperature, precipitation, real evapotranspiration (RET), available water (AW), runoff, SM, TWS, and leaf area index (LAI)—with an emphasis on spatial heterogeneity and extreme event modulation. The aim is to evaluate whether SAI could moderate hydroclimatic extremes in CSATP or instead introduce new challenges, especially in Western Central Asia (WCA), Eastern Central Asia (ECA), the TP, and SA. This regional focus builds on global-scale analyses and contributes new insights into SAI's potential benefits and risks for freshwater systems in one of the world's most vulnerable and water-stressed regions.

https://doi.org/10.5194/egusphere-2025-3493
Preprint. Discussion started: 14 August 2025

2. Data and Methods

2.1 Study area

Geographically, the CSATP stretches from the Caspian Sea in the west to the Xinjiang Uygur Autonomous Region in the northeast, the TP in the east, and the Indo-Gangetic Plain and peninsular India in the south, extending toward the Indian Ocean. The region spans approximately from 8° to 45° N latitude and 40° to 100° E longitude (**Figure 1**). The CSATP comprises Central Asia (CA), SA, and the TP, each with distinct geographical features and contrasting climatic conditions. According to the Intergovernmental Panel on Climate Change (IPCC), CA is further divided into WCA and ECA. The WCA includes countries such as Turkey, Georgia, Armenia, Azerbaijan, Iraq, Iran, Afghanistan, Kyrgyzstan, Kazakhstan, Tajikistan, Uzbekistan, and Turkmenistan. The ECA covers northwestern China, particularly the Xinjiang Uygur Autonomous Region, and includes geographical features such as the Kunlun Mountains, Taklamakan Desert, Gobi Desert, and southern Mongolia. The TP lies directly south of ECA, while SA lies to the south of both WCA and the TP, encompassing southern Pakistan, India, Bangladesh, and Myanmar. The greater Himalayas form a natural climatic and geographical divide between the TP and SA. Collectively, the CSATP represents a highly climate-sensitive and hydro-climatically complex region, increasingly vulnerable to the accelerating impacts of global warming.

2.2 Model simulations and scenarios

In this study, the Community Earth System Model version 2 with the Whole Atmosphere Community Climate Model version 6 component (CESM2 (WACCM6)) is used to simulate hydroclimatic responses under a high-emissions scenario (SSP5-8.5) and a geoengineering scenario (Geo-SAI), enabling detailed assessments of variables including temperature, precipitation, soil and water evaporation, transpiration, SM, TWS, and LAI across the CSATP in future (2071–2100) and present-day conditions (2015-2035). This study utilized simulations from CESM2 (WACCM6), developed by the National Center for Atmospheric Research (NCAR) (Eyring et al., 2016; Rezaei et al., 2024, 2023; Tilmes et al., 2020a). CESM2 (WACCM6) is a fully coupled Earth system model that includes interactive components for atmosphere, ocean, land, and sea ice, and is designed to simulate climate variability and change on a global scale (Gettelman et al., 2019). The model participated in the CMIP6, providing data under various future emission scenarios.

https://doi.org/10.5194/egusphere-2025-3493
Preprint. Discussion started: 14 August 2025

CESM2 has been evaluated against CESM1 and other CMIP5-6 models, and consistently ranks among the top performers across various metrics (Simpson et al., 2020; Magara et al., 2025).

CESM2 demonstrates improved skill in simulating precipitation patterns over arid regions such as CA (Guo et al., 2021), Africa (Mmame et al., 2023), and the middle east and North Africa (MENA) (Rezaei et al., 2024). CESM2 projects about 1 °C more warming than CESM1 under the high-emissions scenario SSP5-8.5, but shows similar temperature outcomes by 2100 under the lower-emissions scenarios SSP2-4.5 and SSP1-2.6 (Duffey and Irvine, 2024; Clark et al., 2023). The CESM2-WACCM model features a high-resolution vertical structure with 70 levels (Keeble et al., 2020), extending from surface pressure (1000 hPa) up to 4.5×10^{-6} hPa, reaching into the lower thermosphere at around 140 km altitude (Meehl et al., 2020). Additionally, its horizontal resolution of 0.9° latitude by 1.25° longitude (approximately 100 km × 140 km at the equator) enables the model to resolve regional climate features and capture complex interactions between the atmosphere and Earth's surface systems (Liang et al., 2022).

The SSP5-8.5-SAI simulation integrates Geo-SAI with the high-emissions scenario SSP5-8.5 aiming to stabilize global mean temperatures at 1.5 °C (Jones et al., 2022), above pre-industrial levels (1850–1900) (Tilmes et al., 2020b). Geo-SAI aims to modify Earth's radiation budget (Reboita et al., 2025), by increasing reflected shortwave radiation (Reboita et al., 2024), and climate models suggest it could reduce global (Richter et al., 2022), and Arctic temperatures while enhancing Northern Hemisphere Sea ice coverage (Wheeler et al., 2025). We used monthly data for TWS, precipitation, temperature, surface runoff, TWS, SM, and RET, and LAI from all five ensemble members (r1 to r5) of the SSP5-8.5 scenario and the three available ensemble members (r1 to r3) of the Geo-SAI scenario. AW is computed using the precipitation minus RET (Rezaei et al., 2025). RET was obtained by adding transpiration, soil and water evaporation data. For the anomaly analysis, we used the ensemble mean of the SSP5-8.5 data over 2015-2035 as a baseline. The GHG and Geo-SAI scenarios were compared for the period 2071–2100 relative to present-day conditions (2015-2035).

https://doi.org/10.5194/egusphere-2025-3493
Preprint. Discussion started: 14 August 2025

2.3 Changes and Shifts in seasonal dynamics

We assessed changes in seasonal amplitude and shifts in peak timing for eight key land-surface variables (temperature, precipitation, RET, AW, runoff, SM, TWS, and LAI) under SSP5-8.5 and Geo-SAI scenarios during 2071–2100, relative to the baseline period (2015–2035). By analyzing the seasonal cycles derived from ensemble-mean monthly anomalies, we identified the timing of annual maxima (peak month) and corresponding amplitude changes. The changes and shifts in seasonal dynamics are assessed using a harmonic regression approach followed by Rezaei et al. (2025). . For each variable and subregion, we identified the timing of the annual peak (P) and amplitude (Amp) of the seasonal cycle to assess the magnitude of intra-annual variability and the timing of maximum seasonal expression. Changes in these metrics are then quantified by comparing historical and future climate scenarios, enabling the assessment of shifts in both the intensity and timing of seasonality The significant differences in variables relative to the baseline period were identified using two-sided t-tests (P<0.05) indicating statistical significance. The WCA region exhibits a unimodal precipitation pattern with two peaks annually, but these peaks have different magnitudes. We, therefore, selected the larger of the two annual peaks for further analysis, which the code correctly identifies and utilizes (**Figure 4-5**).

3. Results

3.1 Average regional hydro-climatic changes

Figure 2 compares projected spatiotemporal mean changes in temperature, precipitation, RET, AW, runoff, SM, TWS, and LAI between the SSP5-8.5 and Geo-SAI scenarios during 2071–2100, relative to present-day conditions (2015-2035), across WCA, ECA, TP, and SA, whereas the corresponding timeseries are shown in **Figure S1-S8**, and associated ensemble mean maps in **Figure S9-S16**. Temperature under SSP5-8.5 exhibits significant increases in all regions (3.60–4.57 K), whereas it significantly reverses under Geo-SAI in all regions, even below the present-day levels (−0.51 to −0.03 K), except SA (**Figure 2a–d**). Precipitation increases significantly under SSP5-8.5 in WCA, ECA, and SA (1.3%–19.1%) and shows an insignificant increase in TP (14.2%). However, Geo-SAI effetely reverses the increases, particularly in ECA and PT where even precipitation is less than present conditions (-6.1%) (**Figure 2e–h**). RET significantly increases under SSP5-8.5 in

https://doi.org/10.5194/egusphere-2025-3493
Preprint. Discussion started: 14 August 2025

WCA, ECA, and TP (8.8%–12.2%) while the increase is insignificant in SA (0.7%). Geo-SAI over-suppresses the RET decreases in all regions (−8.2% to -2.1%), except WCA where RET is at the same level as the present-day level (**Figure 2i–l**). AW under SSP5-8.5 shows significant increases in ECA, TP, and SA (ranging from 6%–71%), while Geo-SAI significantly reverses it in TP, in other regions it is not effective, even in WCA, it over-increases the TWS, helping the water storage conditions (**Figure 2m–p**).

Runoff under SSP5-8.5 increases significantly in all regions (6.3%–20.1%), while Geo-SAI effectively reverses it, particularly in TP and ECA (**Figure 2q–t**). However, the remained runoff increase in SA is still significantly higher (5.0%) than present-day conditions. SM increases under SSP5-8.5 in ECA and SA significantly (1%–3%) while in WCA and TP slightly (0.2%–0.9%). Geo-SAI impacts on SM are heterogenous in different regions, as SM tend to over-increase in WCA, shows insignificant change in ECA and SA, and significantly over-decreases in TP (−6%) (**Figure 2u–x**). TWS shows significant increases in ECA and SA (1.1–3.8%) and an insignificant increase in WCA (0.7%), while TP exhibits a non-significant decrease (−0.3%) under SSP5-8.5. Geo-SAI over-increases TWS in WCA, ECA, and SA (1.2–3.8%), but over-decreases in TP (−0.5%) (**Figure 2y–ab**). The Geo-SAI-induced RET-decrease is statistically significant in ECA and TP. LAI shows significant increases in all regions under SSP5-8.5 (29.6%–67.7%), while Geo-SAI could not suppress this increase, except in TP partially. It even significantly over-increases LAI in WCA and SA (**Figure 2ac–af**).

3.2 Regional amplitude shifts

Figure 3 compares projected seasonal amplitude changes temperature, precipitation, RET, AW, runoff, SM, TWS, and LAI between the SSP5-8.5 and Geo-SAI during 2071–2100, relative to present-day conditions (2015–2035) across WCA, ECA, TP, and SA. With SSP5-8.5, temperature amplitude increases in WCA (3.5%) and SA (1.5%) while decreases in ECA (−1.0%) and TP (−1.9%). Geo-SAI moderates these fluctuations, showing a slight increase in WCA (1.1%) and ECA (2.3%), a significant decrease in SA (−6.6%), and an increase in TP (6.8%) (**Figure 3a–d**). Precipitation amplitude increases significantly under SSP5-8.5 in TP (32%), ECA (15.7%), SA (12.5%), and WCA (9.4%). However, Geo-SAI effectively moderates the amplitude changes, although a remained increase still projected

https://doi.org/10.5194/egusphere-2025-3493
Preprint. Discussion started: 14 August 2025

in ECA (11.5%), SA (3%), TP (4.3%), and WCA (5.6%) (**Figure 3e–h**). Under SSP5-8.5, RET amplitude increases significantly in SA (21.9%) and ECA (2.2%), and insignificantly in WCA (2.5%), while decreasing significantly in TP (−3.3%). Geo-SAI reveres the SSP5-8.5-induced increases in RET amplitudes, particularly in ECA (−4.7%) and TP (−5.3%) where over-decreases the RET amplitude relative to present-day levels (**Figure 3i–l**). However, the RET amplitude in SA is still remained significantly higher (10.4%). The AW amplitude increases significantly under SSP5-8.5, particularly in TP (40.4%) and ECA (20.4%), while Geo-SAI significantly reverses these increases (**Figure 3m–p**), except in WCA where over-increases it.

Runoff amplitude rises significantly under SSP5-8.5 (insignificant in WCA), with pronounced increases in TP (40%) and SA (19.8%), indicating heightened hydrological variability and flood risk. In contrast, Geo-SAI partially reverses the increased runoff amplitudes while increases still persist in ECA (7.5%), TP (3.8%), and SA (3.6%) (**Figure 3q–t**). SM amplitude increases significantly in ECA (9.9%) and slightly in TP (1%) under SSP5-8.5, while in WCA (−5.2%) and SA (−2.8%) show insignificant decreases. Geo-SAI significantly over-increases SM amplitude in WCA (13.6%), ECA (154.3%), and TP (55.7%), reflecting amplified seasonal fluctuations (**Figure 3u–x**), associated with lower temperature and higher precipitation peaks (**Figure S1–2**). The TWS amplitude increased significantly under SSP5-8.5 in all regions (except in WCA), with substantial rises in ECA (22.1%) and TP (12.9%), indicating intensified seasonal variability.

Geo-SAI effectively reverses the amplitude changes in TWS, as it over-decreases TWS amplitude in ECA (−10.2%) and TP (−6.8%), while significantly over-increases in WCA (15.3%) (**Figure 3y–ab**). This suppression could be a result of cooling temperatures, sustained precipitation, higher soil moisture, and increased regional water availability under Geo-SAI (**Figure S1, 2, 4 and 6**). Finally, LAI amplitude increases significantly in all regions under SSP5-8.5, including WCA (55.4%), ECA (18%), TP (34.6%), and SA (48.7%). Geo-SAI is not effective in suppressing LAI amplitude changes except partially in TP (**Figure 3ae**), most probably due to that its hydrology is more temperature controlling, unlike other three regions with precipitation-dependent hydrological system (**Figure 2**). Geo-SAI significantly over-increases this amplitude in WCA (57.8%), SA

https://doi.org/10.5194/egusphere-2025-3493
Preprint. Discussion started: 14 August 2025

(86.2%), and ECA (37%) (**Figure 3ac–af**). However, in TP, the LAI amplitude is still significantly larger than the present conditions (16.1%). Geo-SAI's inability to suppress LAI amplitude stems from cooler temperatures, enhanced precipitation, lower RET, and abundant SM (**Figure S1–8**).

3.3 Seasonality cycle with peak timings

Figure 4 shows the seasonal cycles of temperature, precipitation, RET, and AW, while **Figure 5** presents the seasonal cycles of runoff, SM, TWS, and LAI over WCA, ECA, TP, and SA under SSP5-8.5 and Geo-SAI, relative to present-day conditions (2015–2035).

Under SSP5-8.5, temperature peaks shift earlier in TP by 0.4 months with a 2 K reduction in amplitude, and in SA, the peak advances slightly (0.1 month) with a 2 K amplitude drop. In contrast, Geo-SAI restores peak timing in TP and boosts amplitude by 7 K, while further reducing amplitude by 7 K in SA without affecting timing (**Figure 4a–d**). For precipitation, SSP5-8.5 causes peak advances in WCA (–0.6 months) and ECA (–0.3 months), along with significant amplitude increases in all regions. Geo-SAI reverses the peak shift in WCA, over-shifts it to later in ECA (0.7 months), and reduces amplitude in most regions except TP (**Figure 4e–h**). In the case of RET, SSP5-8.5 increases amplitude in WCA (3 mm) and SA (22 mm) without altering peak timing, whereas Geo-SAI significantly reduces amplitude in all regions, especially ECA and TP (–5 mm each) with stable timing throughout (**Figure 4i–l**). For AW, SSP5-8.5 advances the peak slightly in WCA (0.1 month) with minor amplitude rise, while Geo-SAI delays the peaks in ECA (0.8 months) and TP (0.2 months) and substantially increases TP's amplitude (40 mm) (**Figure 4m–p**).

SSP5-8.5 advances runoff peaks in WCA (–0.1 months), ECA (–0.1), and TP (–0.3), with substantial amplitude increases in ECA (18 mm) and TP (40 mm). In contrast, Geo-SAI restores peak timing in all regions except TP, where it causes a further delay of 0.4 months, and reduces amplitude overall (**Figure 5a–d**). For SM, SSP5-8.5 causes a slight peak delay in ECA (0.8 months), accompanied by notable amplitude increases (10–35 mm across most regions). Geo-SAI further delays peaks in ECA (1 month) and amplifies SM seasonality dramatically, reaching 154 mm in ECA (**Figure 5e–h**). Regarding TWS, SSP5-8.5 does not shift peak timing significantly but increases amplitude across all regions, especially TP (13 mm). Meanwhile, Geo-SAI advances peak timing in TP and SA (–0.3 months each),

https://doi.org/10.5194/egusphere-2025-3493
Preprint. Discussion started: 14 August 2025

raises amplitude in WCA (15 mm), but reduces it in TP (–7 mm) (**Figure 5i–l**). Finally, for LAI, SSP5-8.5 shifts peaks earlier in TP (–0.4 months) and substantially earlier in SA (–2.2 months), with strong amplitude increases, particularly in TP (35 units). Geo-SAI restores peak timing in TP, further delays it in SA (0.5 months), and enhances amplitude consistently across all regions (**Figure 5m–p**).

Under SSP5-8.5, peak timing generally advances across regions, notably in TP and SA, with significant amplitude increases in precipitation, runoff, SM, and LAI, especially in TP and ECA. In contrast, Geo-SAI largely offsets these changes by restoring peak timing and reducing amplitudes in most variables. However, it strongly amplifies SM and LAI seasonality in ECA and TP.

4 Discussion

SAI can mitigate global warming impacts by reducing extreme heat events (Dagon and Schrag, 2017), stabilizing precipitation patterns (Liu et al., 2021), and offsetting temperature rise. It also alters regional hydrological cycles, weakens monsoon systems, and impacts crop yields (e.g., reduced rice, increased maize in China) (Xia et al., 2014). This study assessed the potential impacts of Geo-SAI scenario on offsetting the future changes in TWS, temperature, precipitation, RET, SM, and LAI imposed by the SSP5-8.5 global warming scenarios across the CSATP. Our analysis utilized climate simulations from the CESM2 (WACCM6) model, incorporating three ensemble members for present-day conditions (2015–2035) and projected during 2071–2100, along with five ensemble members for the standalone SSP5-8.5 scenario. Global warming scenarios leads to widespread increases in temperature, precipitation, runoff, and LAI, with pronounced water cycle intensification in ECA and SA (**Figure 2**, **S1-S8**). Temperature increase is evident in Asia (Miao et al., 2020), with pronounced warming in western and SA (Ren et al., 2024; Ullah et al., 2023c), and CA (Miao et al., 2020). Similarly, precipitation increase is evident across Asia (Feng et al., 2014), particularly in western-SA (Xu et al., 2017), and eastern Asia (Ren et al., 2024). Warming-induced increases in evapotranspiration are also projected, especially in east Asia (Ren et al., 2024). However, contrasting trends are evident for SM and TWS, while long-term SM declines in East Asia (Cheng et al., 2015),

https://doi.org/10.5194/egusphere-2025-3493
Preprint. Discussion started: 14 August 2025

and overall decrease in Asia (Berg et al., 2017). TWS has shown declining trends throughout Asia (Pokhrel et al., 2021), and TP (Zhang et al., 2023).

To enhance regional insights, further breakdown of the Geo-SAI impacts across the CSATP reveals spatially varied responses. For instance, Geo-SAI reduces temperature significantly in all regions and mitigates hydrological increases in most areas, but amplifies SM and LAI in some cases, highlighting spatially variable effects (**Figure 2**, **S1-S8**). SAI offsets many greenhouse gas-driven hydrological impacts, boosting water availability in drylands, but it fails to fully restore runoff in wet or cold regions like the Amazon or Siberia due to residual warming, snowmelt loss, and vegetation changes, complicating water management in summer (Rezaei et al., 2025). Similarly, SAI partially offsets mean TWS declines from GHG forcing in wet regions. As explained by Rezaei et al. (2024), the cooling-induced reductions in RET has little effect in drier lands, with extreme TWS excursions reduced though hyper-arid areas like eastern North Africa still experience declining trends under both SAI and high-emission scenarios. These findings also corroborate our results as, Geo-SAI appears to alleviate warming and enhance TWS, potentially supporting agriculture and water infrastructure stability in WCA and ECA. In contrast, while SAI helps reduce temperature stress, it may not sufficiently offset the ongoing TWS decline driven by glacial retreat in the TP.

SA shows promising gains under Geo-SAI through reduced heat extremes and more stable precipitation, which could improve food security and reduce flood risks. This suggests that, despite broader tropical/subtropical trade-offs, SA may experience net positive outcomes from Geo-SAI scenarios intervention. The findings of Abiodun et al. (2021) based on multi-ensemble climate simulation datasets from the Geoengineering Large Ensemble (GLENS, SAI+RCP8.5) Project over Africa, are consistent with those observed in SA in that SAI effectively moderates temperature and PET. However, while the GLENS results indicate that SAI may overcompensate precipitation in the tropics, leading to a net climate water balance deficit, but SA may not experience the same degree of overcorrection. This suggests that Geo-SAI could offer regionally beneficial outcomes for SA, even if it proves less optimal across the broader tropical belt. Another study by Patel et al. (2023) using

https://doi.org/10.5194/egusphere-2025-3493
Preprint. Discussion started: 14 August 2025

simulations from the GLENS project, assessed the potential impact of SAI on temperature and precipitation extremes over South Africa (SAF).

Their results indicate that SAI experiments are often over-effective in offsetting the projected RCP8.5 increases in the frequency of hot extremes (by up to −60%) and in decreasing cold extremes (by up to 10%) across SAF and its climatic zones, relative to present-day conditions (2010–2030). These findings suggest that SAI could lead to over-cooling in SAF. However, the impact of SAI on precipitation extremes is less linear and more spatially variable across the climatic regions. Recent findings of Zhang et al. (2024a) using the GFDL-ESM4.1 model—aiming to restrict global warming to 2.0°C above pre-industrial levels under the CMIP6 overshoot scenario (SSP5-34-OS)—further support the regional variability of SRM impacts. Their simulations showed over 1.5 °C global cooling and reduced precipitation, especially in the Southern Hemisphere, causing a northward shift in tropical rainfall. These results align with GLENS-based evidence of spatially uneven SAI effects. While some tropical regions may face water deficits, SA could still benefit from reduced heat and more stable rainfall under well-planned interventions.

Geo-SAI demonstrates regionally varied impacts across CSATP, effectively reducing temperature and enhancing water availability in many areas, benefiting SA drylands, while being less effective in wet or glacial regions (like the TP) due to residual warming and hydrological complexities. For instance, the persistent declines in TWS, precipitation, AW, SM, and LAI (**Figure 3ae**) in the TP highlight the limited hydrological recovery under Geo-SAI, reinforcing its reduced effectiveness in cold and glacial regions, as Geo-SAI offers substantial mitigation benefits, its effectiveness is not uniform and must be assessed in tandem with local vulnerabilities. In TP, where vegetation is more sensitive to temperature, Geo-SAI offers partial control. But in WCA, ECA, and SA, where hydrology is more precipitation-driven, the climate modifications from Geo-SAI actually enhance vegetation seasonality, leading to significant LAI amplitude increases. (**Figure S1**)

SSP5-8.5 significantly enhances seasonal amplitude in hydroclimatic variables, especially in TWS, AW, runoff, and precipitation, indicating increased seasonality and extremes. Whereas, Geo-SAI generally dampens these changes, reducing amplitudes in TWS, runoff,

https://doi.org/10.5194/egusphere-2025-3493
Preprint. Discussion started: 14 August 2025

RET, and precipitation, but it amplifies SM and LAI, especially in ECA and TP. The hydroclimatic variables such as temperature, precipitation, RET, AW, SM, and TWS are interlinked, and their interactions vary across climatic zones. For instance, temperature governs RET, which in turn influences soil moisture and available water, while precipitation controls surface water inputs and vegetation growth (**Figure S1-S8**). These feedbacks differ regionally, amplifying water loss in drylands like SA and intensifying snowmelt-driven variability in colder regions like TP. Geo-SAI effectively reduces RET amplitude in cooler, temperature-sensitive regions like TP and ECA due to significant cooling and limited water supply, while SA retains high RET amplitude driven by persistent warmth and sufficient hydrological input (Figure S1–S8). Similarly, runoff, is strongly modulated by precipitation, temperature, RET, and SM with high amplitudes under SSP5-8.5, especially in TP due to increased glacier melt and in SA from intensified rainfall (**Figure 3**). Although Geo-SAI mitigates these impacts by lowering temperatures and RET, residual increased precipitation, soil saturation limits, and delayed snowmelt continue to sustain elevated runoff levels in ECA, TP, and SA. Similarly, significant increase SM amplitude in WCA, ECA, and TP, reflecting amplified seasonality under Geo-SAI is associated with lower temperature and higher precipitation peaks (**Figure S1–2**). Moreover, Geo-SAI reverses TWS amplitude changes by significantly reducing them in ECA and TP while over-increasing in WCA, likely due to cooler temperatures, sustained precipitation, elevated soil moisture, and increased water availability; however, it significantly amplifies LAI amplitude in WCA, SA, and ECA, and maintains high levels in TP, driven by similar hydroclimatic conditions, including reduced RET and abundant moisture (**Figure S1–S8**).

Geo-SAI presents a promising strategy to lessen the adverse impacts of global warming in light of increasing hydroclimatic stress (Lee et al., 2023). For instance, rising temperatures and glacial retreat have intensified water scarcity in CA (Miao et al., 2020), which could be mitigated by Geo-SAI through moderating the decline in TWS and alleviating RET stress, thereby promoting more sustainable water availability. Similarly, extreme heat and monsoon variability have heightened threats to agriculture and food security in SA (Ullah et al., 2023b; Ullah et al., 2023a), which could be addressed by Geo-SAI through reducing

https://doi.org/10.5194/egusphere-2025-3493
Preprint. Discussion started: 14 August 2025

temperature extremes and stabilizing precipitation patterns. The findings of Hussain et al. (2025) corroborate the above studies, indicating decrease in temperature (−0.62 °C) and precipitation (−0.02 mm day^{-1}) under Geo-SAI scenarios in SA during 2020–2069. In addition, Geo-SAI can counteract warming-driven shifts in hydrological variables, potentially boosting SM and vegetation cover, which in turn can improve environmental conditions and reduce climate vulnerability across the region (**Figure 2y-af**), consisting with finding for the eastern Middle East (Rezaei et al., 2024). Such changes not only positively influence the climate system but also have significant implications for human health by reducing malaria transmission. For example, Hussain et al. (2024) observed a decline in malaria distribution over SA during 2020–2090 under SAI. Similarly, Carlson et al. (2022) reported that cooling from Geo-SAI could limit malaria expansion into highlands of East Africa by 2070.

SSP5-8.5 causes earlier runoff peaks and greater amplitude in runoff, temperature, SM, and LAI, however Geo-SAI counteracts many of these changes, restoring timing and reducing variability in most hydrological variables. In addition, it substantially amplifies seasonal signals in SM and LAI while moderating those in precipitation and RET. Geo-SAI is projected to significantly influence monsoonal systems, particularly across South and East Asia, where the monsoon is a critical climatic driver (Bal et al., 2019). Several studies suggest that while SAI may moderate global warming, it introduces complex regional hydrological responses (Tan et al., 2024), indicating Geo-SAI may decrease such trends. However, in the ISM region, Geo-SAI is projected to cause marginal surface cooling, alongside enhanced upper- and lower-level circulation (Bhowmick et al., 2021).

Despite these changes, SAI may reduce both mean and extreme summer monsoon precipitation, driven by lower stratospheric warming, weakened subtropical jets, altered wave activities, geopotential anomalies, weakened Asian Summer Monsoon Anticyclone (ASMA), and regional dust effects (Asutosh et al., 2025). Long-term observations also indicate a weakening of the ASMA, largely driven by anthropogenic aerosols, which disrupt meridional temperature gradients across Eurasia (Qie et al., 2025). Additionally, enhanced aerosol optical depth (AOD) from human activities has weakened the East Asian Summer Monsoon by diminishing land-sea temperature and pressure gradients and

https://doi.org/10.5194/egusphere-2025-3493
Preprint. Discussion started: 14 August 2025

reducing evaporation and surface radiation (Lang et al., 2025). On a global scale, SAI's effects vary by hemisphere: tropical SAI suppresses overall precipitation, while Arctic SAI decreases Northern Hemisphere monsoon rainfall by 2.3% and slightly increases Southern Hemisphere monsoon precipitation (Sun et al., 2020). These findings underscore SAI's complex influence on monsoonal dynamics.

Several caveats and cautionary notes apply to our findings. First, the results are based on a single Earth system model (CESM2) and one climate scenario (SSP5-8.5), using three realizations with SAI and five without. Future research should explore alternative SAI strategies and multiple scenarios to assess the sensitivity of outcomes to model and scenario selection. Notably, some SSPs—such as the high-emissions SSP5 or the regional rivalry SSP3—depict undesirable futures with severe climate risks (Macmartin et al., 2022). The specific SAI experiment used here has further limitations: (1) it assumes deployment begins in 2020, which does not reflect any plausible policy pathway, and (2) it relies solely on SSP5-8.5, chosen for its high signal-to-noise ratio rather than real-world likelihood (Burgess et al., 2020). While this setup helps clarify physical responses, it is inconsistent with current mitigation trajectories. Nevertheless, the spatial patterns and direction of hydroclimatic changes under SAI would likely be qualitatively similar in lower-emission scenarios, with the magnitude of impacts scaling with the suppressed warming (Macmartin et al., 2019).

Although Geo-SAI reduces many warming-driven hydroclimate changes in CSATP, it does not fully reverse trends in all regions or variables. This highlights the need for complementary local adaptation strategies (Herbozo et al., 2022). Model limitations also warrant attention. CESM2 performs well relative to its predecessor CESM1 (Danabasoglu et al., 2020), yet its ~1° horizontal resolution may not fully resolve complex topographic or hydrological gradients. Moreover, hydrological responses to SAI are sensitive to both the climate model and the specific deployment strategy (Jones et al., 2018; Bednarz et al., 2023; Laakso et al., 2024; Zhang et al., 2024b; Rezaei et al., 2025). Importantly, runoff responses are closely tied to ET processes. CESM2's CLM5 land model includes sophisticated vegetation–hydrology dynamics, such as plant hydraulics and dynamic stomatal control (Lawrence et al., 2019; Fisher et al., 2019). While this improves physical

https://doi.org/10.5194/egusphere-2025-3493
Preprint. Discussion started: 14 August 2025

realism, CLM5 may overestimate greening and transpiration under elevated CO_2, particularly in moist ecosystems like the Amazon (Cordak et al., 2025), potentially exaggerating runoff declines. Future studies involving model intercomparisons or targeted sensitivity experiments are needed to evaluate the robustness of these hydrological responses under SAI.

5 Conclusion

This study presents a comprehensive assessment of future hydro-climatic seasonality across CSATP under the high-emission SSP5-8.5 and Geo-SAI scenarios using CESM2-WACCM4 outputs. It highlights the considerable potential of Geo-SAI in mitigating the hydroclimatic extremes for temperature, precipitation, RET, AW, runoff, SM, TWS, and LAI under projected high-emissions scenarios in the CSATP region. The Geo-SAI scenarios demonstrate considerable capacity to counteract the hydroclimatic changes induced by elevated GHG concentrations under SSP5-8.5. Owing to its stronger cooling effect, Geo-SAI more effectively restores region-specific hydroclimatic changes under various climatic conditions, particularly amplitude fluctuations, and peak timing patterns across CSATP. These improvements are especially evident in temperature-sensitive (like the TP and SA) regions where Geo-SAI moderate's extreme seasonality and better aligns land–atmosphere processes with present-day baselines.

The projected findings reveal that SSP5-8.5 significantly intensifies hydroclimatic seasonality, particularly in regions such as the TP and SA, with amplified amplitudes in runoff, SM, and LAI, and earlier peak timings in key land-surface variables. In contrast, Geo-SAI mitigates many of these warming-induced changes, especially by reducing the amplitude of temperature, runoff, precipitation, and RET in cooler, temperature-sensitive regions like TP and ECA. In particular, the reduction in TWS decline and RET anomalies across water-stressed regions like CA and SA underscores the potential of Geo-SAI in supporting long-term water resource sustainability. However, regional disparities remain, as improvements in TWS and SM in CA contrast with continued stress in the TP.

https://doi.org/10.5194/egusphere-2025-3493
Preprint. Discussion started: 14 August 2025

However, Geo-SAI also leads to over-amplification in SM and vegetation seasonality in certain regions, notably WCA and ECA, due to increased water availability and reduced evaporative losses. These findings underscore the spatial heterogeneity in Geo-SAI's efficacy, with positive effects in drought-prone zones like SA and WCA, but limited or complex responses in high-altitude or glaciated areas like the TP. Therefore, while Geo-SAI offers a promising supplementary approach to climate mitigation, further research is essential using multi-model ensembles to evaluate unintended side effects and refine region-specific deployment strategies. These findings contribute to a growing body of evidence advocating cautious but proactive exploration of Geo-SAI as part of a diversified climate resilience. Overall, this study highlights the nuanced role of SAI and emphasizes the importance of regionally tailored assessments when evaluating geoengineering as a climate response strategy.

Data availability. The data for CESM2 simulations are publicly available via its website: https://esgf-node.llnl.gov/search/ cmip6/. To access these specific data via the ESGF website use the source ID CESM2-WACCM, experiment ID ssp585, and frequency "mon". The SSP5-8.5-SAI data are freely available at https://www.earthsystemgrid.org/dataset/ucar. cgd.ccsm4.geomip.ssp5.html (https://doi.org/10.26024/t49k-1016).

Author contributions. AH, HL and AR coordinated the analysis, graphics of various figures, and paper preparation. AR, YM and TC conceptualized and prepared the data. HL, PZ, GX and CY contributed to the discussion and writing. HL acquired the funds.

Competing interests. The contact author has declared that none of the authors has any competing interests.

Disclaimer. Publisher's note: Copernicus Publications remains neutral with regard to jurisdictional claims made in the text, published maps, institutional affiliations, or any other geographical representation in this paper. While Copernicus Publications makes every effort to include appropriate place names, the final responsibility lies with the authors.

Acknowledgements. This work was supported in part by National Natural Science Foundation of China (Grant No. 42371337), the Guangdong Basic and Applied Basic Research Foundation (Grant No. 2024A1515011388 and 2023A1515011946) and the Shenzhen Science and Technology Program (Grant No. JCYJ20230808105709020 and JCYJ20240813142621029), the Guangdong Major Project of Basic and Applied Basic Research (Grant No. 2023B0303000017), and the Scientific Foundation for Youth Scholars of Shenzhen University (Grant No. 868-000001032169), and the Moon-Based

https://doi.org/10.5194/egusphere-2025-3493
Preprint. Discussion started: 14 August 2025

Exploration Research Equipment Purchase Project of Development and Reform Commission of Shenzhen Municipality (Grant No. 2106-440300-04-03-901272).

Reference:

Abiodun, B. J., Odoulami, R. C., Sawadogo, W., Oloniyo, O. A., Abatan, A. A., New, M., Lennard, C., Izidine, P., Egbebiyi, T. S., and MacMartin, D. G.: Potential impacts of stratospheric aerosol injection on drought risk managements over major river basins in Africa, Climatic Change, 169, 31, 2021.

Asutosh, A., Tilmes, S., Bednarz, E. M., and Fadnavis, S.: South Asian Summer Monsoon under stratospheric aerosol intervention, npj Climate and Atmospheric Science, 8, 3, 2025.

Bal, P. K., Pathak, R., Mishra, S. K., and Sahany, S.: Effects of global warming and solar geoengineering on precipitation seasonality, Environmental Research Letters, 14, 034011, 2019.

Bala, G., Duffy, P., and Taylor, K.: Impact of geoengineering schemes on the global hydrological cycle, Proceedings of the National Academy of Sciences, 105, 7664-7669, 2008.

Bednarz, E. M., Butler, A. H., Visioni, D., Zhang, Y., Kravitz, B., and MacMartin, D. G.: Injection strategy–a driver of atmospheric circulation and ozone response to stratospheric aerosol geoengineering, Atmospheric Chemistry and Physics, 23, 13665-13684, 2023.

Berg, A., Sheffield, J., and Milly, P. C.: Divergent surface and total soil moisture projections under global warming, Geophysical Research Letters, 44, 236-244, 2017.

Bhowmick, M., Mishra, S. K., Kravitz, B., Sahany, S., and Salunke, P.: Response of the Indian summer monsoon to global warming, solar geoengineering and its termination, Scientific Reports, 11, 9791, 2021.

Burgess, M. G., Ritchie, J., Shapland, J., and Pielke, R.: IPCC baseline scenarios have over-projected CO2 emissions and economic growth, Environmental Research Letters, 16, 014016, 2020.

Carlson, C. J., Colwell, R., Hossain, M. S., Rahman, M. M., Robock, A., Ryan, S. J., Alam, M. S., and Trisos, C. H.: Solar geoengineering could redistribute malaria risk in developing countries, Nature Communications, 13, 2150, 2022.

https://doi.org/10.5194/egusphere-2025-3493
Preprint. Discussion started: 14 August 2025

550 Chen, R., Duan, K., Shang, W., Shi, P., Meng, Y., and Zhang, Z.: Increase in seasonal
551 precipitation over the Tibetan Plateau in the 21st century projected using CMIP6
552 models, Atmospheric Research, 277, 106306, 2022.
553 Cheng, S., Guan, X., Huang, J., Ji, F., and Guo, R.: Long-term trend and variability of soil
554 moisture over East Asia, Journal of Geophysical Research: Atmospheres, 120, 8658-
555 8670, 2015.
556 Cheng, W., MacMartin, D. G., Dagon, K., Kravitz, B., Tilmes, S., Richter, J. H., Mills, M.
557 J., and Simpson, I. R.: Soil moisture and other hydrological changes in a stratospheric
558 aerosol geoengineering large ensemble, Journal of Geophysical Research:
559 Atmospheres, 124, 12773-12793, 2019.
560 Clark, B., Xia, L., Robock, A., Tilmes, S., Richter, J. H., Visioni, D., and Rabin, S. S.:
561 Optimal climate intervention scenarios for crop production vary by nation, Nature
562 Food, 4, 902-911, 2023.
563 Cordak, A. S., Kooperman, G. J., Zarakas, C. M., Swann, A. L., and Koven, C. D.: The
564 role of leaf area changes within plant CO2 physiological impacts on the global
565 hydrological cycle, Geophysical Research Letters, 52, e2024GL110904, 2025.
566 Crutzen, P. J.: Albedo enhancement by stratospheric sulfur injections: a contribution to
567 resolve a policy dilemma?, Climatic change, 77, 211, 2006.
568 Dagon, K. and Schrag, D. P.: Regional climate variability under model simulations of solar
569 geoengineering, Journal of Geophysical Research: Atmospheres, 122, 12,106-
570 112,121, 2017.
571 Dagon, K. and Schrag, D. P.: Quantifying the effects of solar geoengineering on
572 vegetation, Climatic Change, 153, 235-251, 2019.
573 Danabasoglu, G., Lamarque, J. F., Bacmeister, J., Bailey, D., DuVivier, A., Edwards, J.,
574 Emmons, L., Fasullo, J., Garcia, R., and Gettelman, A.: The community earth system
575 model version 2 (CESM2), Journal of Advances in Modeling Earth Systems, 12,
576 e2019MS001916, 2020.
577 Duffey, A. and Irvine, P. J.: Accounting for transience in the baseline climate state changes
578 the surface climate response attributed to stratospheric aerosol injection,
579 Environmental Research: Climate, 3, 041008, 2024.

https://doi.org/10.5194/egusphere-2025-3493
Preprint. Discussion started: 14 August 2025

580 Effiong, U. and Neitzel, R. L.: Assessing the direct occupational and public health impacts
581 of solar radiation management with stratospheric aerosols, Environmental Health, 15,
582 1-9, 2016.
583 Eyring, V., Bony, S., Meehl, G. A., Senior, C. A., Stevens, B., Stouffer, R. J., and Taylor,
584 K. E.: Overview of the Coupled Model Intercomparison Project Phase 6 (CMIP6)
585 experimental design and organization, Geoscientific Model Development, 9, 1937-
586 1958, 2016.
587 Fallah, B., Didovets, I., Rostami, M., and Hamidi, M.: Climate change impacts on Central
588 Asia: Trends, extremes and future projections, International Journal of Climatology,
589 44, 3191-3213, 2024.
590 Feng, S., Hu, Q., Huang, W., Ho, C.-H., Li, R., and Tang, Z.: Projected climate regime
591 shift under future global warming from multi-model, multi-scenario CMIP5
592 simulations, Global and Planetary Change, 112, 41-52, 2014.
593 Fisher, R. A., Wieder, W. R., Sanderson, B. M., Koven, C. D., Oleson, K. W., Xu, C.,
594 Fisher, J. B., Shi, M., Walker, A. P., and Lawrence, D. M.: Parametric controls on
595 vegetation responses to biogeochemical forcing in the CLM5, Journal of Advances in
596 Modeling Earth Systems, 11, 2879-2895, 2019.
597 Gettelman, A., Hannay, C., Bacmeister, J. T., Neale, R. B., Pendergrass, A., Danabasoglu,
598 G., Lamarque, J. F., Fasullo, J., Bailey, D., and Lawrence, D.: High climate sensitivity
599 in the Community Earth System Model version 2 (CESM2), Geophysical Research
600 Letters, 46, 8329-8337, 2019.
601 Guo, H., Bao, A., Chen, T., Zheng, G., Wang, Y., Jiang, L., and De Maeyer, P.: Assessment
602 of CMIP6 in simulating precipitation over arid Central Asia, Atmospheric Research,
603 252, 105451, 2021.
604 Herbozo, J. E., Muñoz, L. E., Guerra, M. J., Minaya, V., Haro, P., Carrillo, V., Manciati,
605 C., and Campozano, L.: Non-stationary hydrological regimes due to climate change:
606 The impact of future precipitation in the spillway design of a reservoir, case study:
607 Sube y Baja Dam, in Ecuador, Atmosphere, 13, 828, 2022.
608 Huang, W., Duan, W., and Chen, Y.: Rapidly declining surface and terrestrial water
609 resources in Central Asia driven by socio-economic and climatic changes, Science of
610 the Total Environment, 784, 147193, 2021.

https://doi.org/10.5194/egusphere-2025-3493
Preprint. Discussion started: 14 August 2025

611 Hussain, A., Khan, M. A., and Shoaib, M.: Impacts of Solar Geoengineering on Malaria
612 Transmission in South Asia, Authorea Preprints, 2024.
613 Hussain, A., Khan, M. A., and Sipra, H.: Impacts of Solar Geoengineering on Projected
614 Climate of South Asia, International Journal of Climatology, 45, e8695, 2025.
615 Huynh, H. N. and McNeill, V. F.: The potential environmental and climate impacts of
616 stratospheric aerosol injection: A review, Environmental Science: Atmospheres, 4,
617 114-143, 2024.
618 Irvine, P. J. and Keith, D. W.: Halving warming with stratospheric aerosol geoengineering
619 moderates policy-relevant climate hazards, Environmental Research Letters, 15,
620 044011, 2020.
621 Ji, D., Fang, S., Curry, C. L., Kashimura, H., Watanabe, S., Cole, J. N., Lenton, A., Muri,
622 H., Kravitz, B., and Moore, J. C.: Extreme temperature and precipitation response to
623 solar dimming and stratospheric aerosol geoengineering, Atmospheric Chemistry and
624 Physics, 18, 10133-10156, 2018.
625 Jones, A., Haywood, J. M., Scaife, A. A., Boucher, O., Henry, M., Kravitz, B., Lurton, T.,
626 Nabat, P., Niemeier, U., and Séférian, R.: The impact of stratospheric aerosol
627 intervention on the North Atlantic and quasi-biennial oscillations in the
628 geoengineering model intercomparison project (GeoMIP) G6sulfur experiment,
629 Atmospheric Chemistry and Physics, 22, 2999-3016, 2022.
630 Jones, A. C., Haywood, J. M., and Jones, A.: Climatic impacts of stratospheric
631 geoengineering with sulfate, black carbon and titania injection, Atmospheric
632 Chemistry and Physics, 16, 2843-2862, 2016.
633 Jones, A. C., Hawcroft, M. K., Haywood, J. M., Jones, A., Guo, X., and Moore, J. C.:
634 Regional climate impacts of stabilizing global warming at 1.5 K using solar
635 geoengineering, Earth's Future, 6, 230-251, 2018.
636 Keeble, J., Hassler, B., Banerjee, A., Checa-Garcia, R., Chiodo, G., Davis, S., Eyring, V.,
637 Griffiths, P. T., Morgenstern, O., and Nowack, P.: Evaluating stratospheric ozone and
638 water vapor changes in CMIP6 models from 1850–2100, Atmospheric Chemistry and
639 Physics Discussions, 2020, 1-68, 2020.

https://doi.org/10.5194/egusphere-2025-3493
Preprint. Discussion started: 14 August 2025

Kim, J.-B. and Bae, D.-H.: Intensification characteristics of hydroclimatic extremes in the Asia monsoon region under 1.5 and 2.0 C of global warming, Hydrology and Earth System Sciences Discussions, 2020, 1-30, 2020.

Kraaijenbrink, P. D., Bierkens, M. F., Lutz, A. F., and Immerzeel, W.: Impact of a global temperature rise of 1.5 degrees Celsius on Asia's glaciers, Nature, 549, 257-260, 2017.

Kravitz, B., Caldeira, K., Boucher, O., Robock, A., Rasch, P. J., Alterskjaer, K., Karam, D. B., Cole, J. N., Curry, C. L., and Haywood, J. M.: Climate model response from the geoengineering model intercomparison project (GeoMIP), Journal of Geophysical Research: Atmospheres, 118, 8320-8332, 2013a.

Kravitz, B., Rasch, P. J., Forster, P. M., Andrews, T., Cole, J. N., Irvine, P. J., Ji, D., Kristjánsson, J. E., Moore, J. C., and Muri, H.: An energetic perspective on hydrological cycle changes in the Geoengineering Model Intercomparison Project, Journal of Geophysical Research: Atmospheres, 118, 13,087-013,102, 2013b.

Laakso, A., Visioni, D., Niemeier, U., Tilmes, S., and Kokkola, H.: Dependency of the impacts of geoengineering on the stratospheric sulfur injection strategy–Part 2: How changes in the hydrological cycle depend on the injection rate and model used, Earth System Dynamics, 15, 405-427, 2024.

Lang, Y., Zhang, J., Zhao, J., Gong, Y., Han, T., Deng, X., and Liu, Y.: Mechanisms and quantification: How anthropogenic aerosols weaken the East Asian summer monsoon, npj Climate and Atmospheric Science, 8, 13, 2025.

Lawrence, D. M., Fisher, R. A., Koven, C. D., Oleson, K. W., Swenson, S. C., Bonan, G., Collier, N., Ghimire, B., Van Kampenhout, L., and Kennedy, D.: The Community Land Model version 5: Description of new features, benchmarking, and impact of forcing uncertainty, Journal of Advances in Modeling Earth Systems, 11, 4245-4287, 2019.

Lee, W. R., MacMartin, D. G., Visioni, D., Kravitz, B., Chen, Y., Moore, J. C., Leguy, G., Lawrence, D. M., and Bailey, D. A.: High-latitude stratospheric aerosol injection to preserve the Arctic, Earth's Future, 11, e2022EF003052, 2023.

Li, X., Long, D., Scanlon, B. R., Mann, M. E., Li, X., Tian, F., Sun, Z., and Wang, G.: Climate change threatens terrestrial water storage over the Tibetan Plateau, Nature Climate Change, 12, 801-807, 2022.

https://doi.org/10.5194/egusphere-2025-3493
Preprint. Discussion started: 14 August 2025

671 Liang, Z., Rao, J., Guo, D., and Lu, Q.: Simulation and projection of the sudden
672 stratospheric warming events in different scenarios by CESM2-WACCM, Climate
673 Dynamics, 59, 3741-3761, 2022.
674 Lin, X., Huang, S., Li, J., Huang, Q., Shi, H., She, D., Leng, G., Wei, X., Guo, W., and
675 Liu, Y.: Feedback dynamics between precipitation, temperature, and soil moisture in
676 China and their possible driving mechanisms under a changing environment,
677 Atmospheric Research, 106983, 2023.
678 Liu, Z., Lang, X., and Jiang, D.: Impact of stratospheric aerosol injection geoengineering
679 on the summer climate over East Asia, Journal of Geophysical Research:
680 Atmospheres, 126, e2021JD035049, 2021.
681 Liu, Z., Lang, X., and Jiang, D.: Stratospheric aerosol injection geoengineering would
682 mitigate greenhouse gas-induced drying and affect global drought patterns, Journal of
683 Geophysical Research: Atmospheres, 129, e2023JD039988, 2024.
684 MacMartin, D., Visioni, D., Kravitz, B., Richter, J., Felgenhauer, T., Lee, W., Morrow, D.,
685 Parson, E., and Sugiyama, M.: Scenarios for modeling solar radiation modification,
686 Proceedings of the National Academy of Sciences, 119, e2202230119, 2022.
687 MacMartin, D. G., Wang, W., Kravitz, B., Tilmes, S., Richter, J. H., and Mills, M. J.:
688 Timescale for detecting the climate response to stratospheric aerosol geoengineering,
689 Journal of Geophysical Research: Atmospheres, 124, 1233-1247, 2019.
690 MacMartin, D. G., Kravitz, B., Tilmes, S., Richter, J. H., Mills, M. J., Lamarque, J. F.,
691 Tribbia, J. J., and Vitt, F.: The climate response to stratospheric aerosol
692 geoengineering can be tailored using multiple injection locations, Journal of
693 Geophysical Research: Atmospheres, 122, 12,574-512,590, 2017.
694 Magara, G., Haque, M., Okrah, A., Nyasulu, M., Yeboah, E., Ebaju, G. K., Akimana, D.,
695 Hasan, T., and Mostahidul Hasan, S.: Evaluating CMIP6 models for CO2 and CH4
696 concentrations across Africa: performance, biases, and implications for climate
697 predictions, Climate Dynamics, 63, 1-18, 2025.
698 Meehl, G. A., Arblaster, J. M., Bates, S., Richter, J. H., Tebaldi, C., Gettelman, A.,
699 Medeiros, B., Bacmeister, J., DeRepentigny, P., and Rosenbloom, N.: Characteristics
700 of future warmer base states in CESM2, Earth and Space Science, 7, e2020EA001296,
701 2020.

https://doi.org/10.5194/egusphere-2025-3493
Preprint. Discussion started: 14 August 2025

Miao, L., Li, S., Zhang, F., Chen, T., Shan, Y., and Zhang, Y.: Future drought in the dry lands of Asia under the 1.5 and 2.0 C warming scenarios, Earth's Future, 8, e2019EF001337, 2020.

Mmame, B., Sunitha, P., Samatha, K., Rao, S., Satish, P., Amasarao, A., and Sekhar, K. C.: Assessment of CMIP6 model performance in simulating atmospheric aerosol and precipitation over Africa, Advances in Space Research, 72, 3096-3108, 2023.

Naumann, G., Cammalleri, C., Mentaschi, L., and Feyen, L.: Increased economic drought impacts in Europe with anthropogenic warming, Nature Climate Change, 11, 485-491, 2021.

Niemeier, U. and Schmidt, H.: Changing transport processes in the stratosphere by radiative heating of sulfate aerosols, Atmospheric Chemistry and Physics, 17, 14871-14886, 2017.

Patel, T. D., Odoulami, R. C., Pinto, I., Egbebiyi, T. S., Lennard, C., Abiodun, B. J., and New, M.: Potential impact of stratospheric aerosol geoengineering on projected temperature and precipitation extremes in South Africa, Environmental Research: Climate, 2, 035004, 2023.

Pokhrel, Y., Felfelani, F., Satoh, Y., Boulange, J., Burek, P., Gädeke, A., Gerten, D., Gosling, S. N., Grillakis, M., and Gudmundsson, L.: Global terrestrial water storage and drought severity under climate change, Nature Climate Change, 11, 226-233, 2021.

Pope, F. D., Braesicke, P., Grainger, R., Kalberer, M., Watson, I., Davidson, P., and Cox, R.: Stratospheric aerosol particles and solar-radiation management, Nature Climate Change, 2, 713-719, 2012.

Qie, K., Tian, W., Bian, J., Xie, F., and Li, D.: Weakened Asian summer monsoon anticyclone related to increased anthropogenic aerosol emissions in recent decades, npj Climate and Atmospheric Science, 8, 140, 2025.

Reboita, M. S., Crespo, N. M., Ribeiro, J. G. M., and da Rocha, R. P.: South Atlantic subtropical anticyclone responses to stratospheric aerosol injection, Environmental Research: Climate, 4, 015003, 2025.

Reboita, M. S., Ribeiro, J. G. M., Crespo, N. M., da Rocha, R. P., Odoulami, R. C., Sawadogo, W., and Moore, J.: Response of the Southern Hemisphere extratropical

https://doi.org/10.5194/egusphere-2025-3493
Preprint. Discussion started: 14 August 2025

cyclone climatology to climate intervention with stratospheric aerosol injection, Environmental research: climate, 3, 035006, 2024.

Ren, Y., Yu, H., Huang, J., Peng, M., and Zhou, J.: The projected response of the water cycle to global warming over drylands in East Asia, Earth's Future, 12, e2023EF004008, 2024.

Rezaei, A., Karami, K., Tilmes, S., and Moore, J. C.: Changes in global teleconnection patterns under global warming and stratospheric aerosol intervention scenarios, Atmospheric Chemistry and Physics, 23, 5835-5850, 2023.

Rezaei, A., Karami, K., Tilmes, S., and Moore, J. C.: Future water storage changes over the Mediterranean, Middle East, and North Africa in response to global warming and stratospheric aerosol intervention, Earth System Dynamics, 15, 91-108, 2024.

Rezaei, A., Moore, J., Tilmes, S., and Karami, K.: Regional and seasonal hydrological changes with and without Stratospheric Aerosol Intervention under High Greenhouse Gas climates, Journal of Geophysical Research: Atmospheres, 130, e2025JD044163, 2025.

Richter, J. H., Visioni, D., MacMartin, D. G., Bailey, D. A., Rosenbloom, N., Dobbins, B., Lee, W. R., Tye, M., and Lamarque, J.-F.: Assessing Responses and Impacts of Solar climate intervention on the Earth system with stratospheric aerosol injection (ARISE-SAI): protocol and initial results from the first simulations, Geoscientific Model Development, 15, 8221-8243, 2022.

Ricke, K., Wan, J. S., Saenger, M., and Lutsko, N. J.: Hydrological consequences of solar geoengineering, Annual review of earth and planetary sciences, 51, 447-470, 2023.

Robock, A., Oman, L., and Stenchikov, G. L.: Regional climate responses to geoengineering with tropical and Arctic SO2 injections, Journal of Geophysical Research: Atmospheres, 113, 2008.

Samaniego, L., Thober, S., Kumar, R., Wanders, N., Rakovec, O., Pan, M., Zink, M., Sheffield, J., Wood, E. F., and Marx, A.: Anthropogenic warming exacerbates European soil moisture droughts, Nature Climate Change, 8, 421-426, 2018.

Schiferl, L. D., Heald, C. L., and Kelly, D.: Resource and physiological constraints on global crop production enhancements from atmospheric particulate matter and nitrogen deposition, Biogeosciences, 15, 4301-4315, 2018.

https://doi.org/10.5194/egusphere-2025-3493
Preprint. Discussion started: 14 August 2025

764 Simpson, I., Tilmes, S., Richter, J., Kravitz, B., MacMartin, D., Mills, M. J., Fasullo, J.,
765 and Pendergrass, A. G.: The regional hydroclimate response to stratospheric sulfate
766 geoengineering and the role of stratospheric heating, Journal of Geophysical Research:
767 Atmospheres, 124, 12587-12616, 2019.
768 Simpson, I. R., Bacmeister, J., Neale, R. B., Hannay, C., Gettelman, A., Garcia, R. R.,
769 Lauritzen, P. H., Marsh, D. R., Mills, M. J., and Medeiros, B.: An evaluation of the
770 large-scale atmospheric circulation and its variability in CESM2 and other CMIP
771 models, Journal of Geophysical Research: Atmospheres, 125, e2020JD032835, 2020.
772 Stevenson, S., Coats, S., Touma, D., Cole, J., Lehner, F., Fasullo, J., and Otto-Bliesner, B.:
773 Twenty-first century hydroclimate: A continually changing baseline, with more
774 frequent extremes, Proceedings of the National Academy of Sciences, 119,
775 e2108124119, 2022.
776 Sun, W., Wang, B., Chen, D., Gao, C., Lu, G., and Liu, J.: Global monsoon response to
777 tropical and Arctic stratospheric aerosol injection, Climate Dynamics, 55, 2107-2121,
778 2020.
779 Tan, M. L., Tew, Y. L., Liew, J., Bala, G., Tye, M. R., Chang, C. K., and Muhamad, N.:
780 Assessment of solar geoengineering impact on precipitation and temperature extremes
781 in the Muda River Basin, Malaysia using CMIP6 SSP and GeoMIP6 G6 simulations,
782 Science of The Total Environment, 948, 174817, 2024.
783 Tilmes, S., MacMartin, D. G., Lenaerts, J., Van Kampenhout, L., Muntjewerf, L., Xia, L.,
784 Harrison, C. S., Krumhardt, K. M., Mills, M. J., and Kravitz, B.: Reaching 1.5 and
785 2.0° C global surface temperature targets using stratospheric aerosol geoengineering,
786 Earth System Dynamics, 11, 579-601, 2020a.
787 Tilmes, S., MacMartin, D. G., Lenaerts, J. T., Van Kampenhout, L., Muntjewerf, L., Xia,
788 L., Harrison, C. S., Krumhardt, K. M., Mills, M. J., and Kravitz, B.: Reaching 1.5 and
789 2.0◦ C global surface temperature targets using stratospheric aerosol geoengineering,
790 Earth System Dynamics, 11, 579-601, 2020b.
791 Tilmes, S., Richter, J. H., Kravitz, B., MacMartin, D. G., Mills, M. J., Simpson, I. R.,
792 Glanville, A. S., Fasullo, J. T., Phillips, A. S., and Lamarque, J.-F.: CESM1
793 (WACCM) stratospheric aerosol geoengineering large ensemble project, Bulletin of
794 the American Meteorological Society, 99, 2361-2371, 2018.

https://doi.org/10.5194/egusphere-2025-3493
Preprint. Discussion started: 14 August 2025

Ullah, I., Zeng, X. M., Mukherjee, S., Aadhar, S., Mishra, A. K., Syed, S., Ayugi, B. O., Iyakaremye, V., and Lv, H.: Future amplification of multivariate risk of compound drought and heatwave events on South Asian population, Earth's Future, 11, e2023EF003688, 2023a.

Ullah, S., You, Q., Ullah, W., Sachindra, D., Ali, A., Bhatti, A. S., and Ali, G.: Climate change will exacerbate population exposure to future heat waves in the China-Pakistan economic corridor, Weather and Climate Extremes, 40, 100570, 2023b.

Ullah, W., Karim, A., Ullah, S., Rehman, A.-U., Bibi, T., Wang, G., Ullah, S., Bhatti, A. S., Ali, G., and Abbas, A.: An increasing trend in daily monsoon precipitation extreme indices over Pakistan and its relationship with atmospheric circulations, Frontiers in Environmental Science, 11, 1228817, 2023c.

Vicente-Serrano, S. M., McVicar, T. R., Miralles, D. G., Yang, Y., and Tomas-Burguera, M.: Unraveling the influence of atmospheric evaporative demand on drought and its response to climate change, Wiley Interdisciplinary Reviews: Climate Change, 11, e632, 2020.

Visioni, D., MacMartin, D. G., Kravitz, B., Richter, J. H., Tilmes, S., and Mills, M. J.: Seasonally modulated stratospheric aerosol geoengineering alters the climate outcomes, Geophysical Research Letters, 47, e2020GL088337, 2020.

Wang, B., Bao, Q., Hoskins, B., Wu, G., and Liu, Y.: Tibetan Plateau warming and precipitation changes in East Asia, Geophysical Research Letters, 35, 2008.

Weisenstein, D. K., Keith, D. W., and Dykema, J.: Solar geoengineering using solid aerosol in the stratosphere, Atmospheric Chemistry and Physics, 15, 11835-11859, 2015.

Wheeler, L., Wagman, B., Smith, W., Davies, P., Cook, B., Brunell, S., Glen, A., Hackenburg, D., Lien, J., and Shand, L.: Design and simulation of a logistically constrained high-latitude, low-altitude stratospheric aerosol injection scenario in the Energy Exascale Earth System Model (E3SM), Environmental Research Letters, 20, 044011, 2025.

Xia, L., Robock, A., Cole, J., Curry, C. L., Ji, D., Jones, A., Kravitz, B., Moore, J. C., Muri, H., and Niemeier, U.: Solar radiation management impacts on agriculture in China: A

https://doi.org/10.5194/egusphere-2025-3493
Preprint. Discussion started: 14 August 2025

case study in the Geoengineering Model Intercomparison Project (GeoMIP), Journal of Geophysical Research: Atmospheres, 119, 8695-8711, 2014.

Xu, Y., Zhou, B.-T., Wu, J., Han, Z.-Y., Zhang, Y.-X., and Wu, J.: Asian climate change under 1.5–4 C warming targets, Advances in Climate Change Research, 8, 99-107, 2017.

Yu, W., Liu, Y., Yang, X.-Q., Wu, G., He, B., Li, J., and Bao, Q.: Impact of North Atlantic SST and Tibetan Plateau forcing on seasonal transition of springtime South Asian monsoon circulation, Climate Dynamics, 56, 559-579, 2021.

Zhang, Q., Shen, Z., Pokhrel, Y., Farinotti, D., Singh, V. P., Xu, C.-Y., Wu, W., and Wang, G.: Oceanic climate changes threaten the sustainability of Asia's water tower, Nature, 615, 87-93, 2023.

Zhang, S., Naik, V., Paynter, D., Tilmes, S., and John, J.: Assessing GFDL-ESM4. 1 climate responses to a stratospheric aerosol injection strategy intended to avoid overshoot 2.0 C warming, Geophysical Research Letters, 51, e2024GL113532, 2024a.

Zhang, Y., MacMartin, D. G., Visioni, D., Bednarz, E. M., and Kravitz, B.: Hemispherically symmetric strategies for stratospheric aerosol injection, Earth System Dynamics, 15, 191-213, 2024b.

Zhu, C., Ullah, W., Wang, G., Lu, J., Li, S., Feng, A., Hagan, D. F. T., Jiang, T., and Su, B.: Diagnosing potential impacts of Tibetan Plateau spring soil moisture anomalies on summer precipitation and floods in the Yangtze River basin, Journal of Geophysical Research: Atmospheres, 128, e2022JD037671, 2023.

Zhu, L., Ju, J., Qiao, B., Liu, C., Wang, J., Yang, R., Ma, Q., Guo, L., and Pang, S.: Physical and biogeochemical responses of Tibetan Plateau lakes to climate change, Nature Reviews Earth & Environment, 1-15, 2025.

https://doi.org/10.5194/egusphere-2025-3493
Preprint. Discussion started: 14 August 2025

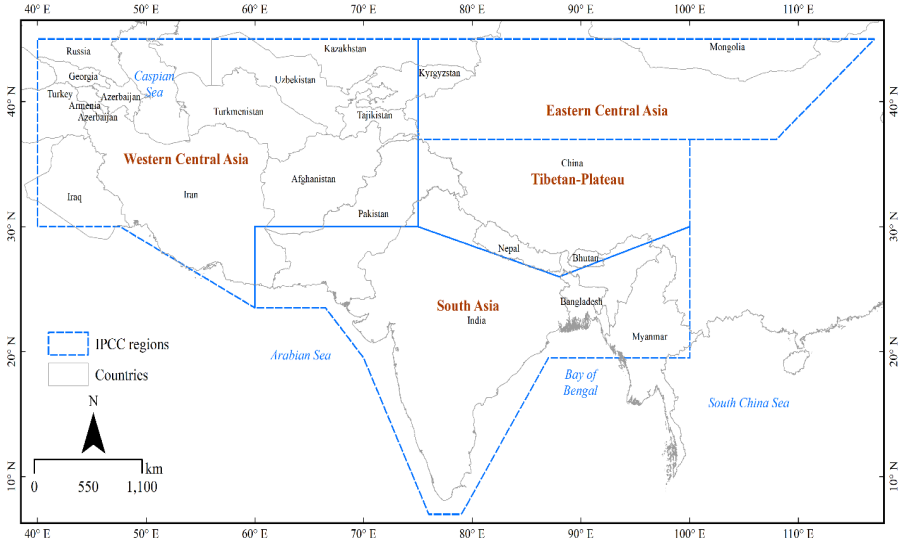

851

852 **Figure 1.** Location map of countries in Asia and in sub-regions as defined by the
853 Intergovernmental Panel on Climate Change (IPCC) working group I (WGI), also known
854 as the IPCC reference regions (V4) in Asia.

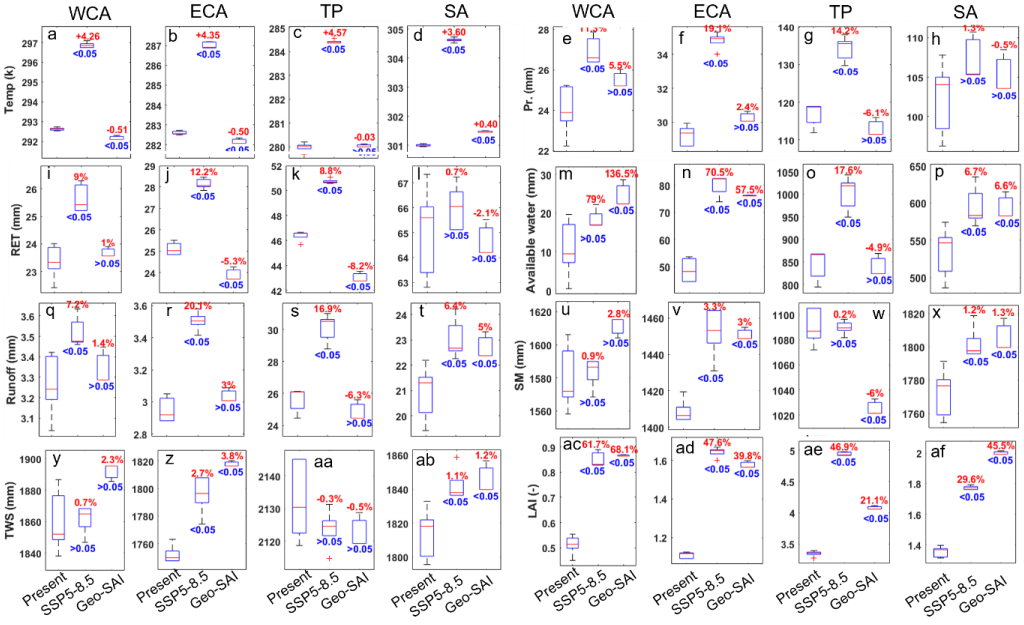

855

856 **Figure 2.** Projected changes in spatiotemporal mean changes in temperature (a–d),
857 precipitation (e–h), real evapotranspiration (RET; i–l), Available water (AW; m–p), runoff
858 (q–t), soil moisture (SM; u–x), terrestrial water storage (TWS; y–aa), and leaf area index

https://doi.org/10.5194/egusphere-2025-3493
Preprint. Discussion started: 14 August 2025

(LAI; ac–af) under present, SSP5-8.5 and Geo-SAI (SSP5-8.5-SAI) geoengineering scenario during 2071–2100, relative to present-day conditions (2015-2035). Box plots illustrate the distribution of ensemble simulations, with red lines showing medians, boxes representing interquartile ranges, and whiskers indicating ensemble spread. Percentage changes are shown relative to the baseline medians. P-values from two-sided t-tests reflect the statistical significance of differences from the baseline, with values $P<0.05$ considered significant.

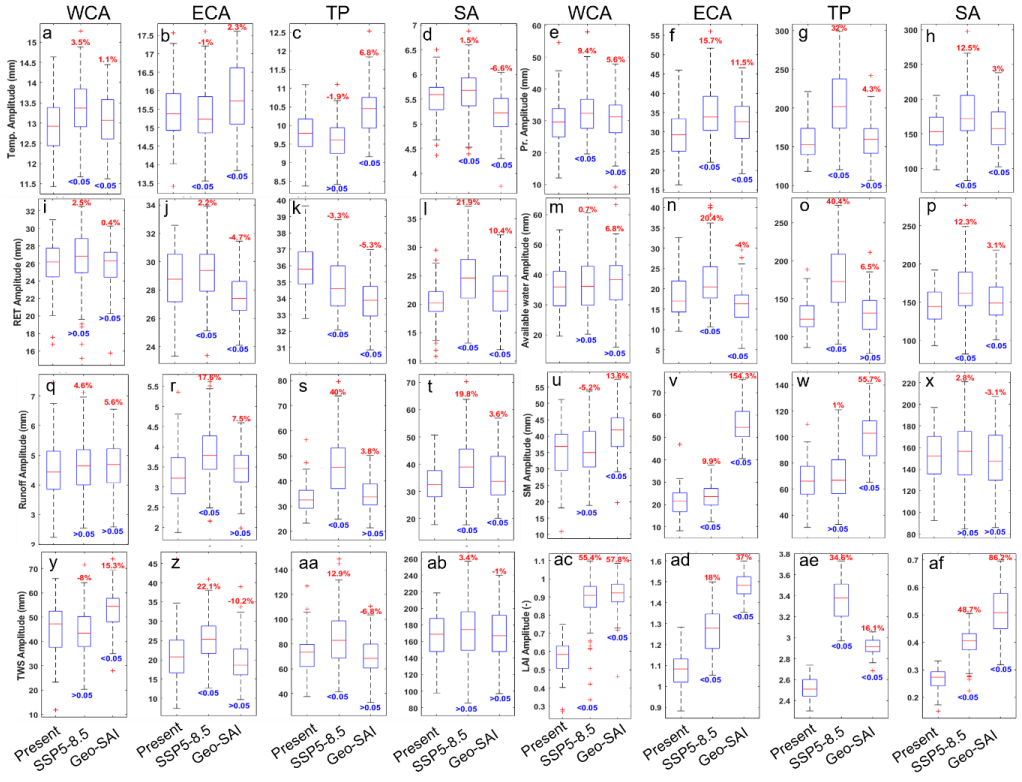

Figure 3. As in Figure 2, but for the amplitude.

https://doi.org/10.5194/egusphere-2025-3493
Preprint. Discussion started: 14 August 2025

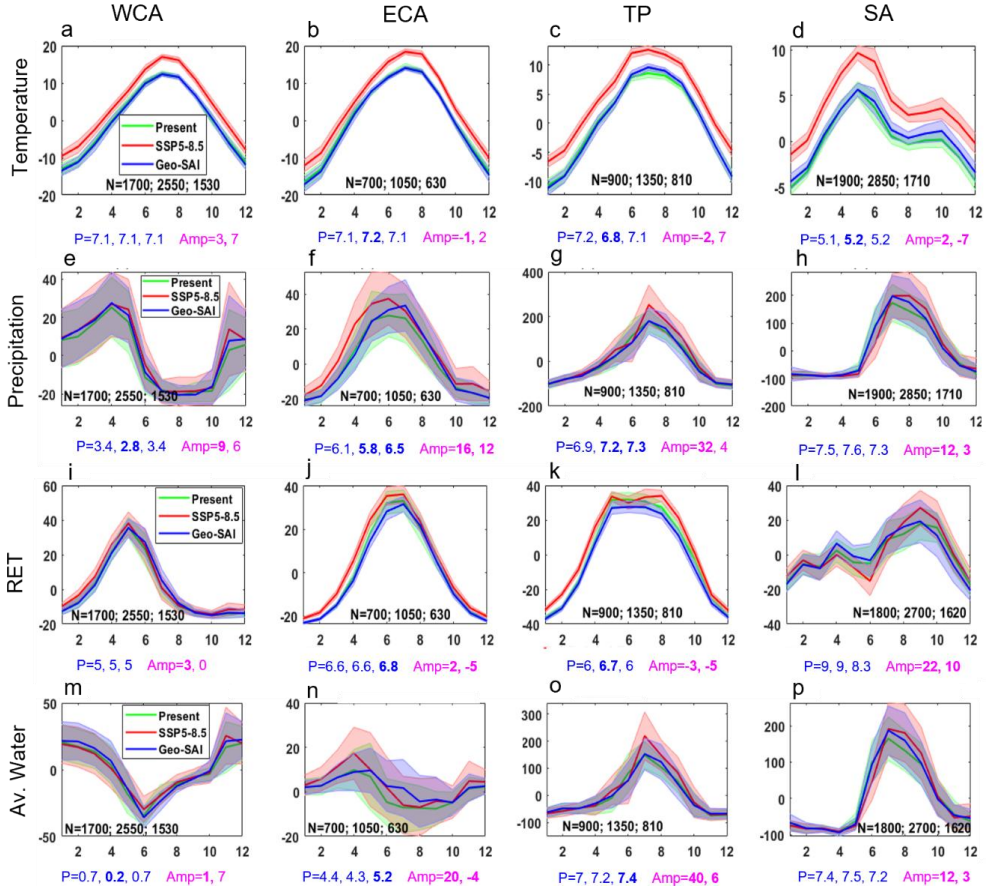

Figure 4. The seasonality cycle of temperature (a–d), precipitation (e–h), RET (i–l) and Av. water (m–p) under SSP5-8.5 and Geo-SAI (2071–2100) relative to the present-day conditions (2015–2035) in WCA, ECA, TP and SA regions. The x-axis is months from January (1) to December (12). Red and blue numbers below each subplot indicate the mean trough (T) and peak (P) month of the annual cycle for present-day, SSP5-8.5, and Geo-SAI. The T shows the trough, P shows the months in which the peak values occur and Amp in pink shows the amplitude changes percentage relative to present. Bold numbers indicate statistically significant shifts/changes (P<0.05 value, t-test) relative to present-day. Three black values (N) in each subplot represent the number of samples used for present-day, SSP5-8.5, and Geo-SAI, respectively, calculated as the product of grid points, years, and ensemble members.

https://doi.org/10.5194/egusphere-2025-3493
Preprint. Discussion started: 14 August 2025

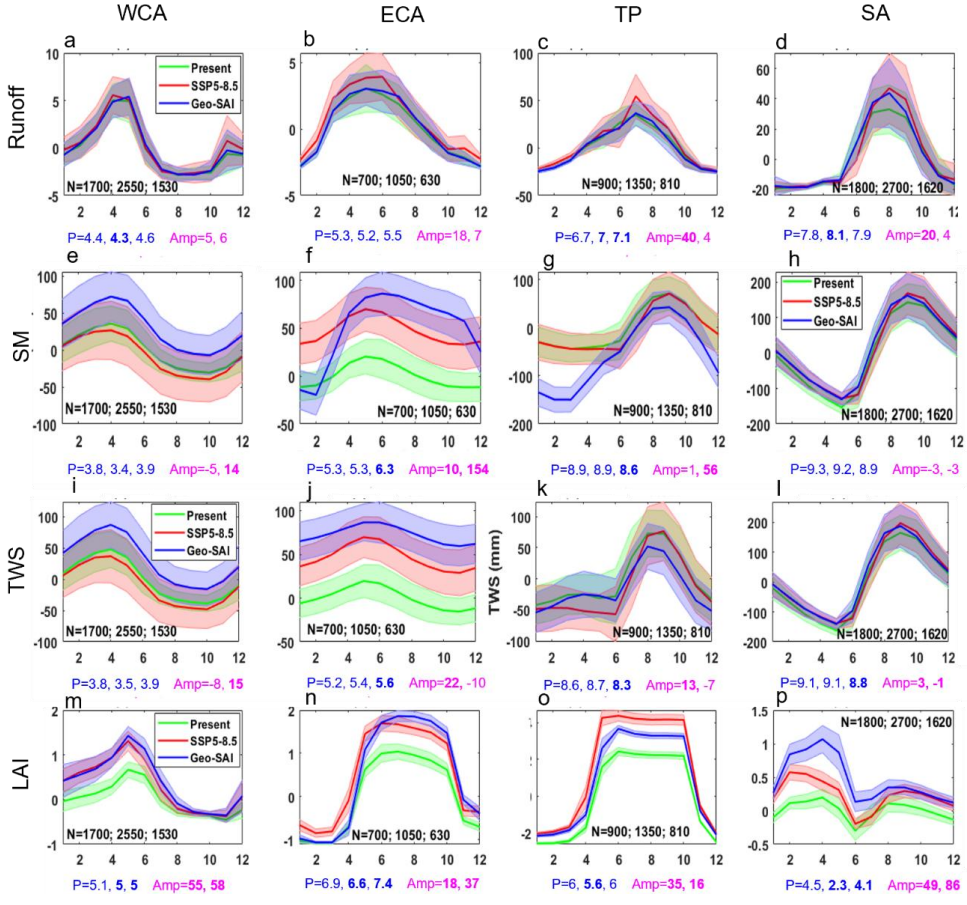

Figure 5. As in Figure 4, but for runoff (a–d), SM (e–h), TWS (i–l) and LAI (m–p).